

Urban sensing as a random search process

Kevin O’Keeffe,¹ Paolo Santi,¹ Brandon Wang,¹ and Carlo Ratti¹

¹*Senseable City Lab, Massachusetts Institute of Technology, Cambridge, MA 02139*

We study a new random search process: the *taxi-drive*. The motivation for this process comes from urban sensing, in which sensors are mounted on moving vehicles such as taxis, allowing urban environments to be opportunistically monitored. Inspired by the movements of real taxis, the taxi-drive is composed of both random and regular parts; passengers are brought to randomly chosen locations via deterministic (i.e. shortest paths) routes. We show through a numerical study that this hybrid motion endows the taxi-drive with advantageous spreading properties. In particular, on certain graph topologies it offers reduced cover times compared to persistent random walks.

I. INTRODUCTION

Random search processes [1–4] are a well studied topic with a bounty of practical applications. Examples include the spreading of diseases and rumours [5], gene transcription [2], animal foraging [6–9], immune systems chasing pathogens [10], robotic exploration [11], and transport in disordered media [12, 13]. Early research on random searches focused on symmetric random walks in Euclidean spaces. Over the years however, many variants have been considered, such as persistent random walks [14–16], intermittent random walks [7, 17, 18], and Levy flights [19–22], each of which offer advantages in certain contexts. Topologies other than Euclidean spaces, such as random graphs or real-world networks, have also been studied [23–25].

Here we explore a new random search process: the *taxi-drive*. As the name suggests, this process models the movement of taxis. The motivation for studying such a process comes from a recent (theoretical) work in urban sensing [26] in which sensors are deployed on taxis, thereby allowing air pollution, road congestion, and other urban phenomena to be monitored ‘parasitically’. As such, this drive-by approach [27–30] to urban sensing can be viewed as a random search process, in which a city’s environment is ‘sensed’ (i.e. searched) by sensor-bearing taxis as they drive around serving passengers.

Similar to Levy walks [19, 20] or the run-and-tumble motion of bacteria [31, 32], the motion of taxis is part-random, part-regular: passenger destinations are chosen randomly, but the routes taken to those destinations are (approximately) deterministic. This mix of ballistic and random motion makes the spreading properties of taxis unusual; as shown in [26] – and reproduced in Figure 2(a) – the stationary distribution of the taxi-drive process on real-world street networks follow Zipf’s law, in agreement with large, real-world taxi data from nine cities worldwide. This behavior is unusual because it differs significantly from that of classic random search process such as the random walk, which, as show Figure 2(b), produces stationary distributions on the same street networks which are skewed and unimodal.

The purpose of this work is to further explore the taxi-drive process. We do not study its ability to capture real-world data; instead, our goal is theoretical: to

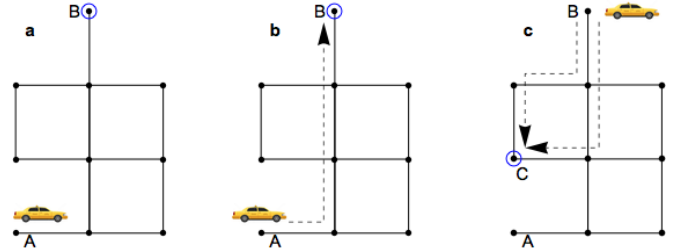


FIG. 1: **The taxi-drive.** (a) A taxi picks up a passenger at node A and a destination node B , circled blue, is randomly chosen. (b) The shortest path between A and B is taken as indicated by the dashed arrow. (c) Now at B , the taxi’s next pickup is at C . There are two shortest paths connecting B and C , so one is chosen at random. This process then repeats.

study the taxi-drive as a stochastic process. We focus on cover times, which we numerically compute and compare to those of other well known stochastic processes, namely the persistent random walk, and the regular random walk. We hope our paper inspires further work on the taxi-drive process, as well as more theoretical interest in urban sensing.

II. MODEL

Model definition. Consider a street network S whose edges represent street segments, and whose nodes represent road intersections. Under the assumption that passengers can only be picked up and dropped off at intersections, nodes represent also possible passenger pickup and dropoff locations. The taxi-drive runs on S , and as depicted in Figure 1, is defined by three steps:

1. A taxi picks up a passenger at node A , who wishes to travel to a randomly chosen node B .
2. The taxi travels along the shortest path from node A to node B at unit speed. In the event of multiple shortest paths between A and B , one is chosen at random.
3. The process then repeats.

In order to capture the behavior of real taxis, the des-

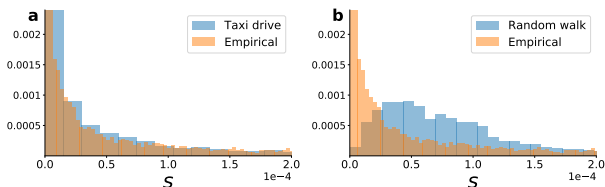


FIG. 2: **Segment popularities.** Histograms of segment popularities s_i , defined as the relative number of times the i -th street segment (represented by edges in the street network) is visited on the Manhattan street network. The Manhattan street network was found using the python package ‘osmnx’. Segment popularity distributions from the taxi-drive process agree well with those obtained from empirical data (panel (a)), whereas those from the random walk do not (panel (b)). The taxi-drive process was run for 10^7 timesteps with $\beta = 1$. Note, this figure is taken from [26] and reproduced here for convenience.

tionation node B is *not* chosen uniformly at random (i.e. in step 2 above). A ‘preferential return mechanism’ is instead required, in which the probability of selecting the n ’th node is $q_n \propto 1 + v_n^\beta$, where v_n is the number of times node n has been previously visited and β is free parameter. Song et al showed this preferential return mechanism captures the statistical properties of human mobility patterns [33], and the authors in [26] show that it also captures the statistics of taxi mobility patterns. In particular, it produces realistic segment popularity distributions, where the i -th segment’s popularity s_i is the relative number of times that segment was visited by a fleet of taxis over a given reference period (note segments are edges in the street network). For convenience, we reproduced the figure in that work in Figure 2 which shows the empirical s_i derived from taxi-data in Manhattan agree well with those obtained from the taxi-drive process when $\beta = 1$. The good agreement is surprising, since the taxi-drive process ignores many complexities affecting the motion of real taxis, such as traffic conditions, variations in drivings speeds and segment lengths, human routing decision, and so on.

In this work however, we are interested in the taxi-drive process from a theoretical stand point. So for simplicity’s sake, we set $\beta = 0$ so that destination nodes are chosen uniformly at random.

Relation to other models. As discussed in the Introduction, the taxi-drive is closely related to the Levy walk. Before showing our results, we contrast the two processes. Like the taxi-drive, Levy walkers travel to randomly chosen destinations at constant speed along a trajectory, but instead of choosing a destination node directly (as the taxi-drive does) the walker jumps a distance r sampled from $P(r) \propto r^{-1-\alpha}$ in a direction chosen uniformly at random. When the Levy walk takes place on a graph – the case we are concerned with in this work – the node nearest to the walkers landing site is chosen as the destination. Thus, the graph on which the Levy walker

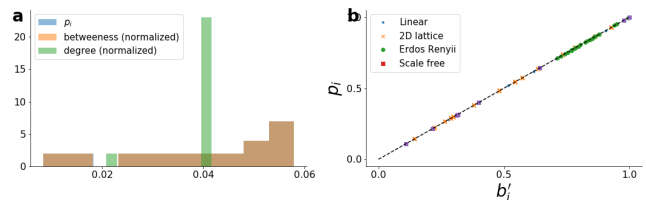


FIG. 3: **Stationary densities** (a) Distributions of p_i , betweenness, and degree for the linear graph, which consists of N nodes arranged in a line with edges between adjacent nodes. We have normalized the betweenness and degree so that their sum is 1. The p_i are distributed similarly to the betweenness (orange and blue shaded areas overlapping perfectly); the p_i are *not* distributed in the same way the degree d_i , as would be expected if the p_i were generated from a random walk. In panel (b) we show $p_i \propto b'_i$ relation for the taxi-drive holds true for other graphs, both regular and random. Note b'_i is the adjusted betweenness as defined by (2). Note also that we have re-scaled by $p_i \rightarrow p_i/p_{i,max}$ and $b_i \rightarrow b'_i/b'_{i,max}$ so that they lie in the interval $[0, 1]$.

moves must be embedded in Euclidean space (although generalizations of Levy-type strategies to networks have been considered [34, 35]). Since the taxi-drive process is not defined in terms of distance, it choosing nodes as destinations directly, it can be applied to graphs with arbitrary topology. (Note, when the taxi-drive chooses shortest path routes to destinations, these shortest paths are calculated with respect to the number of edges, and *not* with respect to a euclidean distance.)

III. RESULTS

A. Stationary densities

We first examine stationary densities of the taxi-drive. We begin with perhaps the simplest topology, namely the linear graph which consists of N nodes arranged in a line with edges between adjacent nodes (i.e a 1D lattice). We ran the taxi-drive until stable conditions are reached, and counted the relative number p_i of times each node was visited. Note that we focus on nodes here, and not edges as was done in Figure 2; edges, corresponding to road segments, were the more natural object to consider in the study of urban sensing [26] from which the figure is taken. On the other hand, our focus here is on stationary properties of the underlying graph exploration process, and node statistics are typically used for this purpose. Figure 3(a) shows a histogram of the values of p_i along with histograms of the values of the betweenness b_i and degree d_i of the nodes in the graph. Interestingly, for the taxi-drive the stationary densities of a given node p_i are distributed similarly to the betweenness b_i . This contrasts with the stationary densities of the random walk, which are proportional to the nodes degree $p_i \propto d_i$.

The relation between the taxi-drive p_i and b_i follows

from the similarities between the taxi-drive and the definition of a node's betweenness b_i , given by

$$b_i := \frac{1}{(N-1)(N-2)} \sum_{s,t,i \neq s,t} \frac{\sigma_{st}(i)}{\sigma_{st}} \quad (1)$$

where N is the number of nodes in the graph, σ_{st} is the number of shortest paths connecting the start node s and end node t , and $\sigma_{st}(i)$ is the number of those paths that contain the node i . Since asymptotically every start-end node combination will be sampled by the taxi-drive, and shortest paths are taken between these start and end nodes, a relationship between b_i and p_i is expected. They are however not precisely equivalent. Notice that the start and end nodes are not included in Eq. (1), as denoted by $i \neq s, t$ in the iterator of the sum. This is what makes $b_i \neq p_i$, since in the taxi-drive destination nodes are 'counted' when they are traversed by the taxi. Origins are however not, since the destination of one trip is the origin of the following trip (note taxis spend just one time unit on each node, and do not 'stall' between dropping off one passenger and picking up another). Hence a minor modification to equation (1)

$$b'_i := \frac{1}{(N-1)(N-2)} \sum_{s,t,i \neq s} \frac{\sigma_{st}(i)}{\sigma_{st}} \quad (2)$$

which we call the adjusted betweenness leads to $b'_i = p_i$. Figure 3(b) shows the relation $b'_i = p_i$ holds true for a variety of different graphs.

B. Cover times

We next investigate the cover times of the taxi-drive process, which leads us to pose the *the curious tourist problem*: A curious tourist arrives in a city. She decides to explore the city by taking taxis to randomly chosen locations. How long does it take her to cover every road at least once?

Due to the non-markovian nature of the taxi-drive (the markovian property is violated since taxis move deterministically when serving passengers), we were unable to solve the curious tourist problem analytically (even for the simple, symmetric random walk exact results for cover times are rare; see [36] for a review). We thus resort to numerical evaluation.

Figure 4 shows how the mean cover time of the taxi-drive $\langle T \rangle_{TD}$ varies with graph size N for the ring (panel (a)) and linear (panel (b)) graphs. For comparison, we also plot the mean cover time for the persistent random walk $\langle T \rangle_{PRW}$. The persistent random walk is a simple extension of the random walk with efficient covering properties [14], and so is a natural baseline for the taxi-drive. It differs from the regular random walk in that at each step the walker's direction of motion persists with

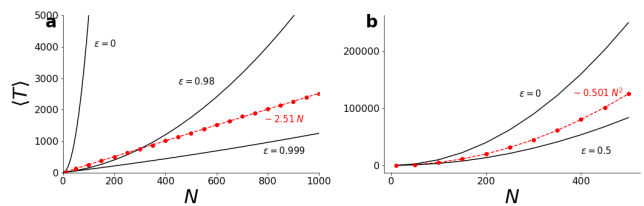


FIG. 4: **Mean cover times on simple graphs.** Red dots show simulation results for the mean cover time of the road-explorer $\langle T \rangle_{RE}$, while the red dashed line shows the lines of best fit to those points. Each data points represents the average of 5000 realizations. Thick black curves show theoretical predictions for the mean cover time of the persistent random walk $\langle T \rangle_{PRW}$ given by Eqs. (3) and (4) (note, the mean cover time of the regular random walk is recovered at $\epsilon = 0$). Panel (a) Ring graph; for all but extreme values of ϵ (i.e. $\epsilon = 0.999$) $\langle T \rangle_{RE} < \langle T \rangle_{PRW}$. As shown by the red text, the line of best fit for the taxi-drive is $\langle T \rangle_{RE} = (2.51 \pm 0.01)N$ (b) Linear graph; $\langle T \rangle_{RE} > \langle T \rangle_{PRW}$ for modest values of ϵ . The line of best fit is given by $\langle T \rangle_{RE} = (0.51 \pm 0.01)N^2$.

probability $(1 - \epsilon)/2$ – and thus a reversal in direction occurs with probability $(1 + \epsilon)/2$ – with $-1 < \epsilon < 1$. Note the regular random walk is recovered at $\epsilon = 0$. Note also that in order for the persistent random walker to be well-defined, the graph on which it is run must be embedded in some 'direction'. The ring and linear graphs have this property, and so the persistent random walk can be run on them (for the linear graph, the boundary conditions are reflective, so that the walker changes direction when these endpoints are reached).

The mean cover times of the persistent random walk on the ring and linear graph are known exactly [37] and are given by

$$\langle T \rangle_{PRW}^{linear} = \frac{1 - \epsilon}{(1 + \epsilon)}(N - 1)(N - 2) + \frac{2}{(1 + \epsilon)}(N - 2) + \frac{2 + \epsilon}{1 + \epsilon} \quad (3)$$

$$\langle T \rangle_{PRW}^{ring} = \frac{1 - \epsilon}{2(1 + \epsilon)}N^2 + \frac{5\epsilon - 1}{2(1 + \epsilon)}N - \frac{2\epsilon}{1 + \epsilon}. \quad (4)$$

From these the mean cover time of the random walk $\langle T \rangle_{RW}$ can be recovered by setting $\epsilon = 0$.

Figure 4 shows that taxi-drive covers the linear and ring graphs more efficiently than the regular random walk ($\epsilon = 0$) for all graph sizes N . For the ring graph (panel (a)), this holds true for the persistent random walk for all but extreme values of ϵ (i.e. $\epsilon \sim 0.999$). The fact that the persistent random walk beats the taxi-drive as $\epsilon \rightarrow 1$ makes sense, because at $\epsilon = 1$ the motion is purely ballistic and trivially covers the ring in $N - 1$ steps (assuming at $t = 0$ the walker has covered the node it starts on, leaving $N - 1$ nodes to be covered). For the linear graph (panel (b)) however the persistent random walk beats the taxi-drive for moderate values of ϵ (i.e. $\epsilon = 0.5$).

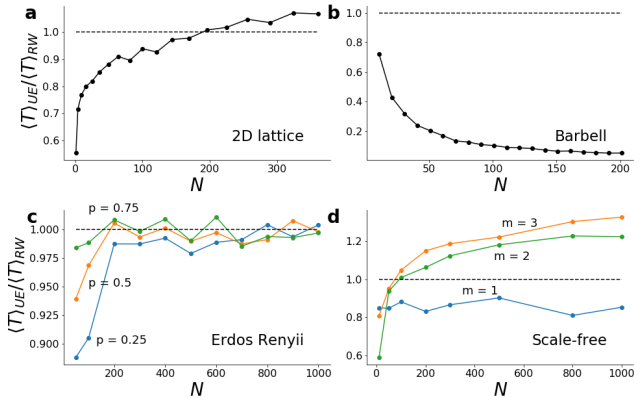


FIG. 5: **Mean cover times on complex graphs.** Dots (both black and colored) represented mean values of ensembles of size 1000. Thick lines simply connect data points. The dashed black line denotes the value 1 and is included to highlight the point at which mean cover time for the random walk $\langle T \rangle_{RW}$ exceeds the mean cover time for the taxi-drive $\langle T \rangle_{TD}$. For each (of 1000) realizations at a given N , a new instance of the random graphs (Erdos-Renyii and scale-free) was realized, which explains the non-monotonicity of the curves. (a) 2D lattice graph (b) Barbell graph, which consists of 2 cliques of size $(N-1)/2$ bridged by a single node. (c) Erdos-Renyii graph with parameter p , defined as the probability of there being an edge between any two nodes. Thus there is a chance that an instance of an Erdos-Renyii graph has more than one connected component, and so in our simulations we took the largest of these. (d) Scale-free graph with parameter m , defined as the number of edges to attach from a new node to existing nodes during the graph growing process.

We next study how $\langle T \rangle_{TD}$ scales as $N \rightarrow \infty$ for the ring and linear graphs. The curves in Figure 4 suggest the scaling might be simple polynomials $\langle T \rangle_{TD} \sim N^a$, so we fit the data to curves of the form $aN^2 + bN$ (the constant term being negligible as $N \rightarrow \infty$). In order for the fitting to be accurate, simulation at large N must be collected. Beyond $N = O(10^4)$ however simulations were prohibitively costly – run times being $O(\text{weeks})$ – so we did not collect data beyond this point. The results of the fitting were

$$\langle T \rangle_{TD}^{linear} = (0.501 \pm 0.001)N^2 + (0 \pm 2)N \quad (5)$$

$$\langle T \rangle_{TD}^{ring} = (10^{-6} \pm 10^{-6})N^2 + (2.52 \pm 0.01)N \quad (6)$$

From these we conjecture

$$\langle T \rangle_{TD}^{linear} \sim O(N^2) \quad (7)$$

$$\langle T \rangle_{TD}^{ring} \sim O(N) \quad (8)$$

Eq. (7) follows from Eq. (5). Eq. (8) follows from Eq. (6); given the closeness of the coefficient of the N^2 term in Eq. (6) to zero we conjecture that $\langle T \rangle_{TD}^{ring} = O(N)$. Of course, since the data these predictions are based on vary

over only four decades, we cannot rule out the presence of higher order terms with small coefficients. Thus we restate that Eq. (7) and Eq. (8) are intended as conjectures, whose proofs are open problems.

We remark that the different scaling properties for the ring and linear graphs are unusual; given the close similarities between the topologies of these graphs, properties of random searches on the graphs (such as cover times $\langle T \rangle$) are typically similar in the $N \rightarrow \infty$ limit.

Next we study cover times on graphs with more complex topology, namely 2D lattices, barbells, Erdos-Renyii, and scale-free graphs. The barbell graph consists of two cliques joined by a single node (variants with more than a single node connecting the two cliques have also been considered). This topology is known to extremize the spreading properties of the random walk [38], so we include it as a baseline. Figure 5 plots the ratio of $\langle T \rangle_{TD}$ to $\langle T \rangle_{RW}$ – that is, compares the taxi-drive and the *regular* random walk only. We do not study the persistent random walk, since it is ill-defined on graphs not embedded in Euclidean spaces, as the aforementioned graphs are [40]. Interestingly, as can be seen in Figure 5, for 2D lattices, Erdos-Renyii, and scale-free graphs below a certain size, the taxi-drive is more efficient than the random walk. This trend appears to hold true for all parameters p of the Erdos-Renyii graphs, and parameters m of the scale-free graphs (see caption of Figure 5 for a definition of these parameters). As expected for the barbell graph, $\langle T \rangle_{TD} < \langle T \rangle_{RW}$ for all graph sizes. The rationale here is that the random walker gets stuck in the bells of the barbell, which the ballistic aspect of the taxi-drive’s movements insulates it from this trapping.

C. m -Cover times

In some random search problems it is desired to cover each node more than once. This is necessary for example in urban sensing, where more than one sample at each spatial location is needed in order to capture the temporal fluctuations of the quantities being measured. This leads us to consider the m -cover time, the time it takes to cover each node at least m times. Thus, we study how the m -cover time of the random walk compared to that of the taxi-drive, and so computed $\langle T \rangle_{TD} / \langle T \rangle_{RW}$ versus m for the six graphs studied so far. We plot the result in Figure 6, which reveals unexpected trends. For the graphs with regular topology – the ring, linear, and 2D lattice – $\langle T \rangle_{TD} / \langle T \rangle_{RW}$ increases with m , eventually crossing the threshold value 1. Yet for the graphs with random topology – the Erdos-Renyii and scale-free – the opposite trend is observed: the taxi-drive beats the random walker as m increases. (The barbell graph is an exception here; it has regular topology, but shows a decline in $\langle T \rangle_{TD} / \langle T \rangle_{RW}$ for increasing m . This isn’t too surprising since as discussed its topology maximizes $\langle T \rangle_{RW}$).

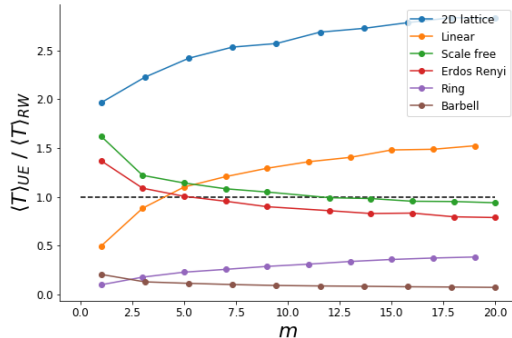


FIG. 6: **m -cover times.** Colored dots represents data points, each of which represents the average of 1000 realizations. Thick lines simple connect data points. The dashed black line denotes 1 and is included to highlight the point at which mean cover time for the random walk $\langle T \rangle_{RW}$ exceeds the mean cover time for the taxi-drive $\langle T \rangle_{TD}$. The parameters for each graph were (i) Ring; $N = 50$ (ii) Linear; $N = 10$ (iii) 2D lattice; $N = 400$ (iv) Barbell; $N = 200$ (v) Erdos-Renyii; $(N, p) = (500, 0.05)$ (vi) Scale-free; $(N, m) = (500, 5)$. The parameters p and m are defined in the caption of Figure 5.

Discussion

Our work shows the taxi-drive is a competitive candidate for random search problems, since it covers graphs more efficiently than the persistent and regular random walk in various contexts. Moreover, the taxi-drive has the benefit of being defined on graphs with arbitrary topology, unlike the persistent random walk, Levy flight, and Levy walk which are confined to graphs embedded in Euclidean space (although as previously mention, generalizations of levy-type strategies to networks have been considered [34, 35])

The taxi-drive could be useful in community detection. Here, efficient algorithms have been designed by exploiting the relationship between the spreading properties of random walkers and graph topology; since the

density $p_i(t)$ of a random walker at a given node is related to its degree d_i , nodes with similar degree – that is, nodes which form some ‘community’ – can be detected by tracking $p_i(t)$ of random walker. By swapping the random walk with the taxi-drive, for which our works shows $p_i(t)$ is related to b_i , perhaps other flavours of community could also be cheaply identified.

Our numerical study of the curious tourist problem raises many questions for future work. First, the conjectured scalings $\langle T \rangle_{TD}^{ring} = O(N)$ and $\langle T \rangle_{TD}^{linear} = O(N^2)$ cry out for theoretical explanation. Second, and more ambitiously, one expects that given the simpleness of the ring and linear graphs that an exact solution for $\langle T \rangle_{TD}$ might be findable. Perhaps the techniques used in [37] to calculate $\langle T \rangle_{PRW}$ could be useful for this purpose. Another interesting open problem is to determine which graph topology maximizes the cover time of the taxi-drive. The ‘stickiness’ of the bells in the barbell graph trap the random walker – what counterpart to this graph motif is needed to hamper the taxi-drive? Lastly, the puzzling behavior of the m -cover time begs explanation. Why does, as our work suggests, the the regularity / randomness of the graph topology determine the scaling of $\langle T \rangle_{TD} / \langle T \rangle_{RW}$ with m ? We hope future work will solve these puzzles, as well as investigate other properties and applications of the taxi-drive.

Source code for the taxi-drive is available under the M.I.T. licence and can be found at [39].

Acknowledgments

The authors would like to thank Allianz, Amsterdam Institute for Advanced Metropolitan Solutions, Brose, Cisco, Ericsson, Fraunhofer Institute, Liberty Mutual Institute, Kuwait-MIT Center for Natural Resources and the Environment, Shenzhen, Singapore- MIT Alliance for Research and Technology (SMART), UBER, Vitoria State Government, Volkswagen Group America, and all the members of the MIT Senseable City Lab Consortium for supporting this research.

-
- [1] S. Condamin, O. Bénichou, V. Tejedor, R. Voituriez, and J. Klafter, *Nature* **450**, 77 (2007).
 - [2] O. Bénichou and R. Voituriez, *Physics Reports* **539**, 225 (2014).
 - [3] S. Redner, *A guide to first-passage processes* (Cambridge University Press, 2001).
 - [4] V. Méndez, D. Campos, and F. Bartumeus, in *Stochastic foundations in movement ecology* (Springer, 2014), pp. 177–205.
 - [5] A. L. Lloyd and R. M. May, *Science* **292**, 1316 (2001).
 - [6] G. M. Viswanathan, M. G. Da Luz, E. P. Raposo, and H. E. Stanley, *The physics of foraging: an introduction to random searches and biological encounters* (Cambridge University Press, 2011).
 - [7] O. Bénichou, C. Loverdo, M. Moreau, and R. Voituriez, *Reviews of Modern Physics* **83**, 81 (2011).
 - [8] G. M. Viswanathan, V. Afanasyev, S. Buldyrev, E. Murphy, P. Prince, and H. E. Stanley, *Nature* **381**, 413 (1996).
 - [9] F. Bartumeus, M. G. E. da Luz, G. M. Viswanathan, and J. Catalan, *Ecology* **86**, 3078 (2005).
 - [10] M. L. Heuzé, P. Vargas, M. Chabaud, M. Le Berre, Y.-J. Liu, O. Collin, P. Solanes, R. Voituriez, M. Piel, and A.-M. Lennon-Duménil, *Immunological reviews* **256**, 240 (2013).
 - [11] M. Vergassola, E. Villermaux, and B. I. Shraiman, *Nature* **445**, 406 (2007).
 - [12] S. Havlin and D. Ben-Avraham, *Advances in Physics* **36**,

- 695 (1987).
- [13] D. Ben-Avraham and S. Havlin, *Diffusion and reactions in fractals and disordered systems* (Cambridge university press, 2000).
- [14] V. Tejedor, R. Voituriez, and O. Bénichou, *Physical review letters* **108**, 088103 (2012).
- [15] P. Cénac, A. Le Ny, B. de Loynes, and Y. Offret, *Journal of Theoretical Probability* **31**, 232 (2018).
- [16] L. Basnarkov, M. Mirchev, and L. Kocarev, in *International Conference on ICT Innovations* (Springer, 2017), pp. 102–111.
- [17] G. Oshanin, H. Wio, K. Lindenberg, and S. Burlatsky, *Journal of Physics: Condensed Matter* **19**, 065142 (2007).
- [18] M. Azaïs, S. Blanco, R. Bon, R. Fournier, M.-H. Pillot, and J. Gautrais, *PLOS ONE* **13**, e0206817 (2018).
- [19] M. F. Shlesinger, J. Klafter, and B. J. West, *Physica A: Statistical Mechanics and its Applications* **140**, 212 (1986).
- [20] A. Blumen, G. Zumofen, and J. Klafter, *Physical Review A* **40**, 3964 (1989).
- [21] G. Viswanathan, V. Afanasyev, S. V. Buldyrev, S. Havlin, M. Da Luz, E. Raposo, and H. E. Stanley, *Physica A: Statistical Mechanics and its Applications* **282**, 1 (2000).
- [22] M. A. Lomholt, K. Tal, R. Metzler, and K. Joseph, *Proceedings of the National Academy of Sciences* (2008).
- [23] J. D. Noh and H. Rieger, *Physical review letters* **92**, 118701 (2004).
- [24] T. Weng, J. Zhang, M. Small, B. Harandizadeh, and P. Hui, *Physical Review E* **97**, 032320 (2018).
- [25] N. Masuda, M. A. Porter, and R. Lambiotte, *Physics reports* (2017).
- [26] K. P. O’Keeffe, A. Anjomshoaa, S. H. Strogatz, P. Santi, and C. Ratti, *arXiv preprint arXiv:1811.10744* (2018).
- [27] U. Lee and M. Gerla, *Computer Networks* **54**, 4 (2010).
- [28] B. Hull, V. Bychkovsky, Y. Zhang, K. Chen, M. Goraczko, A. Miu, E. Shih, H. Balakrishnan, and S. Madden, in *Proceedings of the 4th international conference on Embedded networked sensor systems* (2006), p. 125138.
- [29] P. Mohan, V. N. Padmanabhan, and R. Ramjee, in *Proceedings of the 6th ACM conference on Embedded network sensor systems* (2008), p. 323336.
- [30] A. Anjomshoaa, F. Duarte, D. Rennings, T. Matarazzo, P. de Souza, and C. Ratti, *IEEE Internet of Things Journal* pp. 1–1 (2018).
- [31] M. J. Schnitzer, *Physical Review E* **48**, 2553 (1993).
- [32] H. C. Berg, *E. coli in Motion* (Springer Science & Business Media, 2008).
- [33] C. Song, T. Koren, P. Wang, and A.-L. Barabási, *Nature Physics* **6**, 818 (2010).
- [34] A. P. Riascos and J. L. Mateos, *Physical Review E* **86**, 056110 (2012).
- [35] Q. Guo, E. Cozzo, Z. Zheng, and Y. Moreno, *Scientific reports* **6**, 37641 (2016).
- [36] M. Abdullah, *arXiv preprint arXiv:1202.5569* (2012).
- [37] M. Chupeau, O. Bénichou, and R. Voituriez, *Physical Review E* **89**, 062129 (2014).
- [38] G. Brightwell and P. Winkler, *Random Structures & Algorithms* **1**, 263 (1990).
- [39] https://github.com/Khev/the_taxi_drive.
- [40] The exception being the 2D lattice; persistent random walks have been generalized two dimensional spaces, but require an additional parameter to specify which direction is chosen when the walk changes its direction of motion. We wished to avoid this complication, so do not study this case